ARTICLE NO. 80-4122

# Halo Orbit Formulation for the ISEE-3 Mission

David L. Richardson*
*University of Cincinnati, Cincinnati, Ohio*

**The path to which the ISEE-3 satellite is controlled is a periodic solution to the three-dimensional equations for motion about the interior libration point of the sun-Earth-satellite three-body system. These particular periodic "halo" orbits are constructed using analytical and numerical methods. The third-order analytical solution is obtained by application of successive approximations in conjunction with a form of the Lindstedt-Poincaré method. The ISEE-3 mission orbit is one member of a family of orbits which are locally approximated by the analytical development. This orbit is produced from standard differential corrections procedures using the third-order solution as the initial approximation.**

## I. Introduction

ON August 12, 1978, the International Sun-Earth Explorer satellite, ISEE-3, was launched. One hundred and two days later, the spacecraft was injected into a quasiperiodic orbit about the location of the sun-Earth interior libration point $L_1$. Because of the inherent instability of periodic orbits in the neighborhood of the collinear points, an orbital maintenance strategy must be employed. The stationkeeping strategy involves controlling the satellite to a halo orbit which is of sufficient amplitude to satisfy certain mission constraints. The proper orbit was selected from a halo family of three-dimensional $L_1$-periodic orbits of the circular-restricted problem. By use of successive approximations, this family was constructed analytically through third order and is valid for a certain bounded region of the $L_1$ point. The analytical solution was used by mission design personnel to study the characteristics of $L_1$ halo orbit solutions. The actual mission orbit was constructed numerically using a differential correction procedure designed to adjust the halo orbits produced by the analytical approximation.

Any halo orbit can be characterized completely by specifying a particular out-of-ecliptic plane amplitude $A_z$ of the solution to the linearized equations of motion. Both the analytical and numerical developments employ this identifying scheme. The ISEE-3 spacecraft was targeted to a halo orbit corresponding to an $A_z$ amplitude of

$$A_z = 110{,}000 \text{ km} \tag{1}$$

Projections of this orbit onto the various planes formed by the libration-centered coordinate system are shown in Fig. 2. The coordinate orientation is depicted in Fig. 1: The $x$-$y$ plane coincides with the ecliptic plane with the positive $x$ axis pointing along the line of syzygy away from the sun. The $z$ axis completes this right-handed coordinate system. The three-dimensional equations of motion and their analytical and numerical solutions are expressed in terms of these coordinates.

## II. Expansion of the Nonlinear Equations

The equations of motion for the satellite moving in the vicinity of the interior collinear point can be obtained from the usual equations found in Ref. 1 by translating the origin of coordinates to the location of the interior collinear point $L_1$. However, some computational facility can be obtained if the equations are developed following a Lagrangian mechanics approach to the problem. It has been shown by Richardson[2,3] that the Lagrangian for the motion about any of the three collinear points of the circular-restricted problem has a form nearly identical to that which is obtained for third-body-perturbed two-body motion. The Lagrangian is

$$L = \tfrac{1}{2}(\dot{\boldsymbol{\rho}}\cdot\dot{\boldsymbol{\rho}}) + GE\left[\frac{1}{|\boldsymbol{r}_E-\boldsymbol{\rho}|} - \frac{\boldsymbol{r}_E\cdot\boldsymbol{\rho}}{|\boldsymbol{r}_E|^3}\right] + GS\left[\frac{1}{|\boldsymbol{r}_S-\boldsymbol{\rho}|} - \frac{\boldsymbol{r}_S\cdot\boldsymbol{\rho}}{|\boldsymbol{r}_S|^3}\right] \tag{2}$$

where $\boldsymbol{\rho}$ is the position vector of the satellite relative to the libration point:

$$\boldsymbol{\rho} = x\hat{i} + y\hat{j} + z\hat{k} \tag{3}$$

The quantities $GE$ and $GS$ are the gravitational constants of the Earth and sun, respectively.† The vectors $\boldsymbol{r}_E$ and $\boldsymbol{r}_S$ are the position vectors of the Earth and Sun with respect to the libration point. It is seen from this equation that the $GE$ and $GS$ terms in the right-hand sides have a form that is identical to the expressions obtained if the influence of the Earth and sun were considered as third-body perturbations of a Keplerian orbit about the libration point. This particular structure of the Lagrangian expedites its expansion inasmuch as there exists a considerable body of literature concerning various approaches to the development of the third-body disturbing function. By using a method described in Ref. 5, the Lagrangian can be expressed quite compactly as a power series in the distance $\rho$:

$$L = \tfrac{1}{2}(\boldsymbol{\rho}^*\cdot\boldsymbol{\rho}^*) + \sum_{n\geq 2} c_n \rho^n P_n(\alpha) \tag{4}$$

where the quantity $P_n(\alpha)$ is the $n$th Legendre polynomial of the first kind having an argument $\alpha$ of

$$\alpha = x/\rho \tag{5}$$

Presented at the AAS/AIAA Astrodynamics Specialist Conference, Provincetown, Mass., June 25-27, 1979; submitted July 10, 1979; revision received March 6, 1980. 

Index categories: Analytical and Numerical Methods; Earth-Orbital Trajectories; Spacecraft Dynamics and Control.

*Assistant Professor of Applied Mechanics, Dept. of Aerospace Engineering and Applied Mechanics.

†Farquhar[4] has shown that the accuracy of the sun-Earth circular-restricted model can be enhanced if $L_1$ is defined along the line between the sun and the Earth-moon barycenter. The actual $GE$ factor includes the mass of the moon.

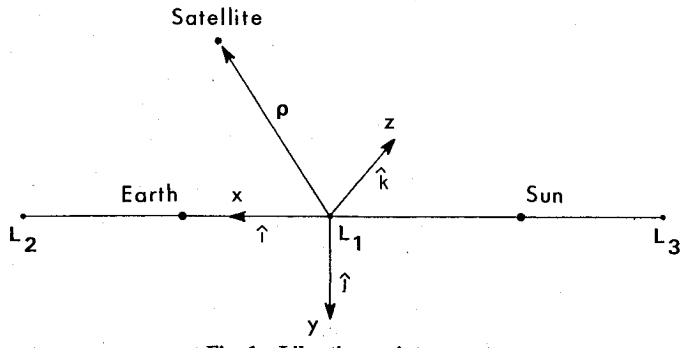


**Fig. 1 Libration-point geometry.**

The application of Lagrange's equations produces the following expressions for the full three-dimensional equations of motion:

$$x^{**}-2y^{*}-(1+2c_2)x=\sum_{n\geq 2}(n+1)c_{n+1}\rho^{n}P_n(\alpha) \tag{6a}$$

$$y^{**}+2x^{*}+(c_2-1)y=\sum_{n\geq 3}c_n y\rho^{n-2}\tilde{P}_n(\alpha) \tag{6b}$$

$$z^{**}+c_2 z=\sum_{n\geq 3}c_n z\rho^{n-2}\tilde{P}_n(\alpha) \tag{6c}$$

where, in the last two equations, the quantity $\tilde{P}_n(\alpha)$ denotes the sum

$$\tilde{P}_n(\alpha)=\sum_{k=0}(3+4k-2n)P_{n-2k-2}(\alpha) \tag{7}$$

The summation is terminated at the first term with a negative subscript. The asterisks in these equations denote differentiation with respect to a nondimensional independent variable $s$ defined through the relationship

$$s=n_E t \tag{8}$$

where $n_E$ is the orbital mean motion of the Earth.

The constants $c_n$ are given by

$$c_n=\frac{1}{\gamma_L^3}\left[\mu+(-1)^n\frac{(1-\mu)\gamma_L^{n+1}}{(1-\gamma_L)^{n+1}}\right] \tag{9}$$

where

$$\mu=GE \tag{10}$$

with the dimensionless quantity $\gamma_L$ defined as the ratio

$$\gamma_L=r_E/a \tag{11}$$

where $a$ is the astronomical unit. The unit of distance is chosen to be the $L_1$-Earth distance $r_E$. The units of mass and time follow from Kepler's third law for the sun-Earth motion by selecting

$$G(E+S)=1 \tag{12}$$

These expressions for the equations of motion are in an ideal form from the point of view that all orders of the nonlinear expansion can be developed recursively using the well-known Legendre polynomial relationships. This is particularly useful if the successive approximation solution procedure is carried to high orders via algebraic manipulation software programs.

## III. Periodic Solutions

The periodic nature of the solution can be seen by considering the linearized form of the equations of motion. They

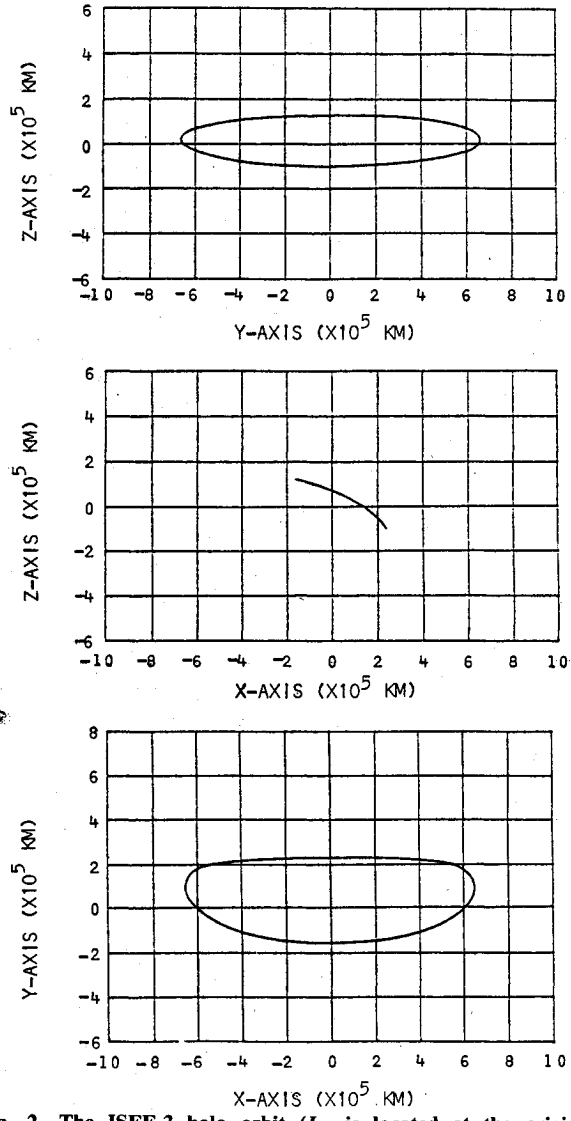


**Fig. 2 The ISEE-3 halo orbit ($L_1$ is located at the origin of coordinates).**

are as follows:

$$x^{**}-2y^{*}-(1+2c_2)x=0 \tag{13a}$$

$$y^{**}+2y^{*}+(c_2-1)y=0 \tag{13b}$$

$$z^{**}+c_2 z=0 \tag{13c}$$

The solution to the characteristic equations for the $x$-$y$ (ecliptic plane) motion has two real and two imaginary roots. As is known, the two real roots are of opposite sign and, consequently, arbitrarily chosen initial conditions will give rise to unbounded motion as time increases. If, however, the initial conditions are restricted so that only the nondivergent mode is allowed, the $x$-$y$ solution can be expressed in the form

$$x=-A_x\cos(\lambda s+\phi) \tag{14a}$$

$$y=kA_x\sin(\lambda s+\phi) \tag{14b}$$

The out-of-plane linearized motion is simply-harmonic and is expressed as

$$z=A_z\sin(\nu s+\psi) \tag{14c}$$

Accordingly, the three-dimensional linearized motion will be quasiperiodic inasmuch as the in-plane and out-of-plane

frequencies $\lambda$ and $\nu$, respectively, are generally unequal.‡ The projections of the motion onto the various coordinate planes produce Lissajous-type trajectories. Using the linearized Lissajous equations as an intermediate orbit on which to build higher-order successive approximations corrections would be unacceptable in view of the ISEE-3 mission constraints (see Refs. 6 and 7). In particular, the motion must be such that the spacecraft will never be seen to traverse any portion of the radio disk of the sun. This constraint is necessary so that solar interference can be eliminated in data transmission between satellite and ground.

Periodic motion which avoids the solar radio disk can be obtained if the amplitudes of the in-plane and out-of-plane motions are of sufficient magnitude so that the nonlinear contributions to the system produce eigenfrequencies that are equal. This condition leads to the so-called halo orbit solution. With this assumption, the linearized equations are rewritten as

$$x^{**}-2y^{*}-(1+2c_2)x=0 \tag{15a}$$

$$y^{**}+2x^{*}+(c_2-1)y=0 \tag{15b}$$

$$z^{**}+\lambda^2 z=0 \tag{15c}$$

where $\lambda^2$ has replaced the coefficient $c_2$ in Eq. (13c). Their solution is

$$x=-A_x\cos(\lambda s+\phi) \tag{16a}$$

$$y=kA_x\sin(\lambda s+\phi) \tag{16b}$$

$$z=A_z\sin(\lambda s+\phi) \tag{16c}$$

where $k$ is a constant given by

$$k=(1/2\lambda)(\lambda^2+1+2c_2) \tag{17}$$

These expressions constitute the generating orbit for the construction of halo-type periodic solutions.

By forcing the linearized $z$ equation to the form of Eq. (15c), it becomes necessary to introduce a correction $\Delta$,

$$\Delta=\lambda^2-c_2 \tag{18}$$

on the right-hand side of Eq. (6c) when higher-order approximations are constructed. The new $z$ equation then becomes

$$z^{**}+\lambda^2 z=\sum_{n\geq 3} c_n z\rho^{n-2}\tilde{P}_n(\alpha)+\Delta z \tag{19}$$

It is easily shown that for motion about $L_1$ in the sun-Earth system that $\Delta$ should obey the order-of-magnitude relation

$$\Delta=0.29221 \quad \text{(normalized units)} \triangleq O(A_z^2) \tag{20}$$

Accordingly, the $\Delta z$ contribution to the solution will first appear in the expressions for the third-order corrections.

A third-order periodic solution to Eqs. (6a), (6b), and (19) is developed using the method of successive approximations in conjunction with techniques similar to the classical approach of the method of Lindstedt-Poincaré: To help remove secular terms, a new independent variable $\tau$ and a frequency correction $\omega$ are introduced via the relation

$$\tau=\omega s \tag{21}$$

where

$$\omega=1+\sum_{n\geq 1}\omega_n \qquad (\omega_n<1) \tag{22}$$

‡Ratios of $\lambda/\nu$ for which the quotient is an integer unequal to one are not considered.

**Table 1 Halo orbit analytical solution parameters**

| | | | |
|---|---|---|---|
| $\mu$ | $3.040357143\times10^{-6}$ | $a_{31}$ | $7.938201951\times10^{-1}$ |
| $\gamma_L$ | $1.001090475\times10^{-2}$ | $a_{32}$ | $8.268538529\times10^{-2}$ |
| $\lambda$ | 2.086453455 | $b_{21}$ | $-4.924458751\times10^{-1}$ |
| $\nu$ | 2.0152105515 | $b_{22}$ | $6.074646717\times10^{-2}$ |
| $\Delta$ | $2.9221445425\times10^{-1}$ | $b_{31}$ | $8.857007762\times10^{-1}$ |
| $c_2$ | 4.0610735668 | $b_{32}$ | $2.301982738\times10^{-2}$ |
| $c_3$ | 3.0200105081 | $d_{21}$ | $-3.468654605\times10^{-1}$ |
| $c_4$ | 3.0305378797 | $d_{31}$ | $1.904387005\times10^{-2}$ |
| $k$ | 3.2292680962 | $d_{32}$ | $3.980954252\times10^{-1}$ |
| $a_{21}$ | 2.092695581 | $s_1$ | $-8.246605235\times10^{-1}$ |
| $a_{22}$ | $2.482976703\times10^{-1}$ | $s_2$ | $1.210986087\times10^{-1}$ |
| $a_{23}$ | $-9.059647954\times10^{-1}$ | $l_1$ | $-1.596559878\times10^{1}$ |
| $a_{24}$ | $-1.044641164\times10^{-1}$ | $l_2$ | 1.740900546 |

Note: mean motion, $n_E=1.990986606\times10^{-7}$ rad/s; astronomical unit $=1.495978714\times10^{8}$ km; unit of distance, $r_E=1.497610042\times10^{6}$ km; unit of time $=5.030853327\times10^{3}$ s.

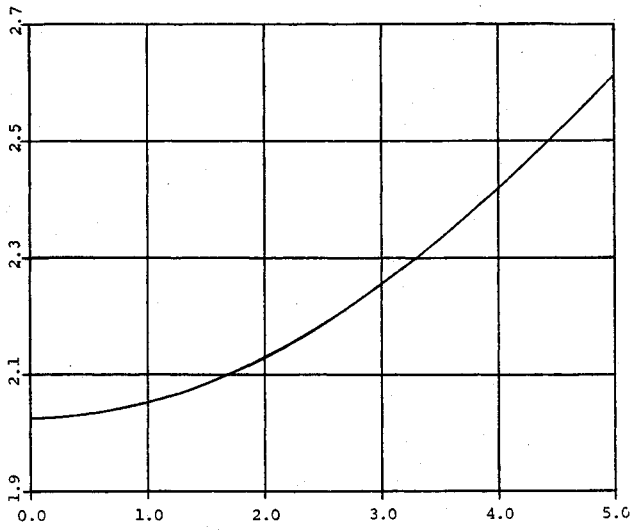


**Fig. 3 Amplitude-constraint relationship.**

The $\omega_n$ are assumed to be of order $A_z^n$ and are chosen to remove the secular terms as they appear during the course of the development of the successive approximation solution. It is found that

$$\omega_1=0 \tag{23a}$$

and

$$\omega_2=s_1A_x^2+s_2A_z^2 \tag{23b}$$

The constants $s_1$ and $s_2$ are complicated expressions involving $\lambda$ and can be found in Refs. 2 and 8.

However, not all of the secular terms can be removed in this manner. Additionally, it becomes necessary to specify amplitude and phase-angle constraint relationships. These expressions are:

$$l_1A_x^2+l_2A_z^2+\Delta=0 \tag{24a}$$

$$\psi-\phi=m\pi/2 \qquad (m=1,3) \tag{24b}$$

The constants $l_1$ ($<0$) and $l_2$ ($>0$) are also lengthy expressions and can be found in the above-cited references. Figure 3 shows the amplitude-constraint relationships for halo-type motion about the sun-Earth $L_1$ point. For the nominal orbit ($A_z=110{,}000$ km), the $x$-axis amplitude is:

$$A_x\cong 206{,}000 \text{ km} \tag{25}$$

This value corresponds to a $y$-axis amplitude of

$$A_y \triangleq kA_x \cong 665{,}000 \text{ km} \tag{26}$$

By use of Eqs. (23b) and (24a), the halo orbit period $T$,

$$T = 2\pi/\lambda\omega n_E \qquad \text{(normalized units)} \tag{27}$$

can be computed as a function of $A_z$. These results are shown in Fig. 4. For the nominal amplitude, the ISEE-3 spacecraft has a period of 177.73 days.

The complete third-order periodic solution was easily constructed using a set of algebraic manipulation subroutines developed by Dasenbrock.[9] The results are as follows

$$x = a_{21}A_x^2 + a_{22}A_z^2 - A_x\cos\tau_1 + (a_{23}A_x^2 - a_{24}A_z^2)\cos 2\tau_1 + (a_{31}A_x^3 - a_{32}A_xA_z^2)\cos 3\tau_1 \tag{28a}$$

$$y = kA_x\sin\tau_1 + (b_{21}A_x^2 - b_{22}A_z^2)\sin 2\tau_1 + (b_{31}A_x^3 - b_{32}A_xA_z^2)\sin 3\tau_1 \tag{28b}$$

$$z = A_z\cos\tau_1 + d_{21}A_xA_z(\cos 2\tau_1 - 3) + (d_{32}A_zA_x^2 - d_{31}A_z^3)\cos 3\tau_1 \tag{28c}$$

where $\tau_1$ denotes the quantity

$$\tau_1 = \lambda\tau + \phi$$

Values for the various constants ($a_{21}$, $b_{21}$, $d_{21}$, etc.) are given in Table 1. The halo orbits corresponding to this solution are shown in Fig. 2.

This set of equations represents one of the two branches of periodic orbits which occur as a result of a bifurcation of the three-dimensional solution. This is described in Refs. 2 and 8. The two branches are viewed as mirror reflections of each other about the $x$-$y$ plane. The nominal orbit corresponds to the branch that Farquhar and Kamel[10] describe as type class I. The solution bifurcation manifests itself through the phase-angle constraint relationship, Eq. (24b). Selecting $m = 1$ in that equation gives the class I orbits, while $m = 3$ produces halo orbits of the second branch (class II).

The stationkeeping strategy for the mission is primarily dependent upon maintaining the orbital stability of the spacecraft in a neighborhood of the nominal path. To this end, the shape of the halo orbit as determined by Eqs. (28) is of particular importance. The accuracy to which the third-order solution represents the orbital shape is determined by the convergence characteristics of the successive approximation development. For relatively small-amplitude halo orbits (as is the nominal orbit), higher-order corrections produce relatively small changes in the features of the orbit. It is shown in the following section that these "small changes" are as much as several thousand kilometers.

## IV. Differentially Corrected Halo Orbits

To ascertain the effects of higher-order corrections on the halo orbits, a differential corrections scheme was developed to produce these periodic orbits numerically. Once the appropriate initial conditions for a particular periodic orbit have been determined, then, through numerical integration, the orbit itself is known and can be expressed as the series

$$x = \sum_{n\geq 0} a_n\cos(n\Omega t) \tag{29a}$$

$$y = \sum_{n\geq 1} b_n\sin(n\Omega t) \tag{29b}$$

$$z = \sum_{n\geq 0} c_n\cos(n\Omega t) \tag{29c}$$

where the constants $a_n$, $b_n$, $c_n$, and the frequency $\Omega$ are implicit functions of $A_z$ which are found to an accuracy of 10-12 significant digits (Table 2). Comparison of these expressions with those of Eqs. (28) reveal small but significant differences in the state variables at various positions along the orbit. For the nominal orbit, the maximum differences in the coor-

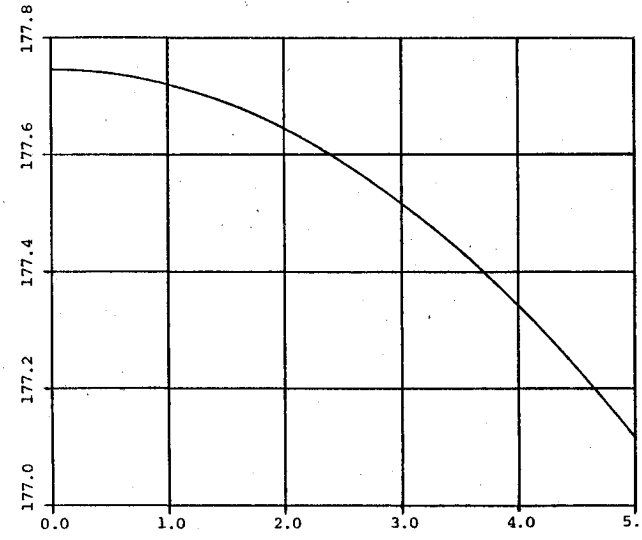


**Fig. 4 Halo-orbit period vs amplitude.**

**Table 2 Normalized nominal-orbit Fourier coefficients**

| | | | | | |
|---|---|---|---|---|---|
| $a_0 = 4.171707420$ | $\times 10^{-2}$ | $b_1 = -4.484081031$ | $\times 10^{-1}$ | $c_0 = 1.214891697$ | $\times 10^{-2}$ |
| $a_1 = 1.413504302$ | $\times 10^{-1}$ | $b_2 = -9.50339473$ | $\times 10^{-3}$ | $c_1 = -7.453756189$ | $\times 10^{-2}$ |
| $a_2 = -1.677812049$ | $\times 10^{-2}$ | $b_3 = -2.32126927$ | $\times 10^{-3}$ | $c_2 = -3.86723856$ | $\times 10^{-3}$ |
| $a_3 = -2.03450790$ | $\times 10^{-3}$ | $b_4 = -3.8869432$ | $\times 10^{-4}$ | $c_3 = -6.0942221$ | $\times 10^{-4}$ |
| $a_4 = -4.1981341$ | $\times 10^{-4}$ | $b_5 = -8.119012$ | $\times 10^{-5}$ | $c_4 = -1.0128761$ | $\times 10^{-4}$ |
| $a_5 = -8.197628$ | $\times 10^{-5}$ | $b_6 = -1.712258$ | $\times 10^{-5}$ | $c_5 = -1.989277$ | $\times 10^{-5}$ |
| $a_6 = -1.759025$ | $\times 10^{-5}$ | $b_7 = -3.80550$ | $\times 10^{-6}$ | $c_6 = -4.09716$ | $\times 10^{-6}$ |
| $a_7 = -3.86475$ | $\times 10^{-6}$ | $b_8 = -8.6531$ | $\times 10^{-7}$ | $c_7 = -8.9001$ | $\times 10^{-7}$ |
| $a_8 = -8.7795$ | $\times 10^{-7}$ | $b_9 = -2.0141$ | $\times 10^{-7}$ | $c_8 = -1.9931$ | $\times 10^{-7}$ |
| $a_9 = -2.0354$ | $\times 10^{-7}$ | $b_{10} = -4.766$ | $\times 10^{-8}$ | $c_9 = -4.581$ | $\times 10^{-8}$ |
| $a_{10} = -4.806$ | $\times 10^{-8}$ | $b_{11} = -1.144$ | $\times 10^{-8}$ | $c_{10} = -1.074$ | $\times 10^{-8}$ |
| $a_{11} = -1.151$ | $\times 10^{-8}$ | $b_{12} = -2.78$ | $\times 10^{-9}$ | $c_{11} = -2.56$ | $\times 10^{-9}$ |
| $a_{12} = -2.79$ | $\times 10^{-9}$ | $b_{13} = -6.8$ | $\times 10^{-10}$ | $c_{12} = -6.2$ | $\times 10^{-10}$ |
| $a_{13} = -6.8$ | $\times 10^{-10}$ | | | $c_{13} = -1.5$ | $\times 10^{-10}$ |

Note: The frequency $\Omega$ is 2.053567977 rad/s.

dinates were found as follows:

$$\Delta x_{\max} = 6641 \text{ km} \quad \Delta y_{\max} = 7468 \text{ km} \quad \Delta z_{\max} = 3909 \text{ km} \tag{30}$$

The halo orbit period is in agreement with that computed from Eq. (13) to an accuracy of approximately 3 h. All discrepancies in position are seen to be of order $A_z^4$, which is consistent with the truncation error of the third-order development. The error in the halo period is also of order $A_z^4$, which is consistent with the level of approximation of the frequency correction $\omega$.

Stationkeeping simulations using a complete dynamical model were conducted to determine fuel costs for controlling the satellite to the third-order path and to the numerically produced orbit. A slight reduction in fuel expenditure was found if the spacecraft were maintained in the vicinity of the differentially corrected solution. The halo orbit solution expressed by Eqs. (29) was, therefore, chosen as the nominal orbit.

The mathematical structure of the differential corrections scheme was dictated in part by the choice of an acceptable out-of-plane displacement $z_0$ necessary to satisfy the radio-disk avoidance constraint. The procedure was therefore required to provide the initial conditions for a halo orbit which passes through the $x$-$z$ plane at $z_0$. One-half period later the orbit must again intersect the $x$-$z$ plane at a displacement which was to be greater than $z_0$. These considerations were implemented as follows. From the third-order equations, the initial estimate for the state vector is determined:

$$\left.\begin{array}{ll} x = x_0, & \dot{x} = 0 \\ y = 0, & \dot{y} = \dot{y}_0 \\ z = z_0, & \dot{z} = 0 \end{array}\right\} \text{ with half-period } T_{1/2} \tag{31}$$

Since the circular-restricted equations of motion admit solutions which are symmetric with respect to the $x$-$z$ plane, then the initial values $x_0$, $\dot{y}_0$, and $T_{1/2}$ can be adjusted so that at the new half-period, the solution path will pass perpendicularly through the $x$-$z$ plane. These adjustments are expressed by the relations

$$x_0 \to x_0 + \Delta x_0 \qquad \dot{y}_0 \to \dot{y}_0 + \Delta \dot{y}_0 \qquad T_{1/2} \to T_{1/2} + \Delta T_{1/2} \tag{32}$$

The half-period boundary conditions for periodicity take the form

$$\dot{x}(x_0 + \Delta x_0, \dot{y}_0 + \Delta \dot{y}_0, T_{1/2} + \Delta T_{1/2}) = 0 \tag{33a}$$

$$\dot{z}(x_0 + \Delta x_0, \dot{y}_0 + \Delta \dot{y}_0, T_{1/2} + \Delta T_{1/2}) = 0 \tag{33b}$$

$$y(x_0 + \Delta x_0, \dot{y}_0 + \Delta \dot{y}_0, T_{1/2} + \Delta T_{1/2}) = 0 \tag{33c}$$

These equations are expanded through first-order in the corrections and are solved to give the matrix equation

$$\begin{bmatrix} \Delta x_0 \\ \Delta \dot{y}_0 \\ \Delta T_{1/2} \end{bmatrix} = -\Phi^{-1} \begin{bmatrix} \dot{x}(x_0, \dot{y}_0, T_{1/2}) \\ \dot{z}(x_0, \dot{y}_0, T_{1/2}) \\ y(x_0, \dot{y}_0, T_{1/2}) \end{bmatrix} \tag{34}$$

where $\Phi$ is the matrix of partials

$$\Phi = \left\{ \begin{array}{ccc} \frac{\partial \dot{x}}{\partial x_0} & \frac{\partial \dot{x}}{\partial \dot{y}_0} & \frac{\partial \dot{x}}{\partial T_{1/2}} \\ \frac{\partial \dot{z}}{\partial x_0} & \frac{\partial \dot{z}}{\partial \dot{y}_0} & \frac{\partial \dot{z}}{\partial T_{1/2}} \\ \frac{\partial y}{\partial x_0} & \frac{\partial y}{\partial \dot{y}_0} & \frac{\partial y}{\partial T_{1/2}} \end{array} \right\}_{t = T_{1/2}} \tag{35}$$

By applying Eqs. (34) and (32) in an iterative fashion with the third-order solution as the initial approximation, the differential corrections converge to improved values for $x_0$, $\dot{y}_0$, $T_{1/2}$ in three or four iterations. In this manner, the nominal orbit initial state was determined, and the results are as follows:

$$\begin{array}{ll} x_0 = 2.452044207 \times 10^5 \text{ km} & \dot{x}_0 = 0.0 \\ y_0 = 0.0 & \dot{y}_0 = -2.917555907 \times 10^2 \text{ m/s} \\ z_0 = -1.003274912 \times 10^5 \text{ km} & \dot{z}_0 = 0.0 \end{array} \tag{36a}$$

The period $T$ is

$$T = 2T_{1/2} = 177.8642659 \text{ days} \tag{36b}$$

The Fourier series expressions of Eqs. (29) were developed through $n = 13$. This level of approximation was determined by the limits on the accuracy of the numerical technique that generated the Fourier coefficients. By specifying that each of the state variables $q_i$ is to be expressible in the form

$$q_i = \frac{a_0^{(i)}}{2} + \sum_{n \geq 1} \left[ a_n^{(i)} \cos\left(\frac{2n\pi}{T} t\right) + b_n^{(i)} \sin\left(\frac{2n\pi}{T} t\right) \right] \tag{37}$$

then the Fourier coefficients are found from the usual relations

$$a_n^{(i)} = \frac{2}{T} \int_0^T q_i \cos\left(\frac{2n\pi}{T} t\right) dt \tag{38a}$$

$$b_n^{(i)} = \frac{2}{T} \int_0^T q_i \sin\left(\frac{2n\pi}{T} t\right) dt \tag{38b}$$

The integrations in these two expressions were performed by using Simpson's composite method[11] with a step size chosen so that the error in the approximation was less than $10^{-10}$. Values for $q_i$ were obtained from a numerical integration of the circular-restricted equations of state using the halo orbit initial conditions as determined by the differential corrections scheme.

## V. Perturbations of the Nominal Orbit

The relatively large excursions of the spacecraft from the $L_1$ point [see Eqs. (25) and (26)] amplifies the effects of the perturbations on the satellite's motion. The most important effects are due to 1) the eccentricity of the Earth's orbit and 2) the gravitational action of the moon. For the nominal amplitude of 110,000 km, eccentricity and lunar action contribute disturbances whose magnitudes are of third and fourth order, respectively. These perturbations are not large, but they must be actively balanced by stationkeeping maneuvers at regular intervals during the mission lifetime.

Solar radiation pressure and planetary perturbations are of small significance. Their contributions are several orders of magnitude less than the effects due to eccentricity. Most of the radiation pressure influence can be modeled through an adjustment of the location of the $L_1$ point. The new location is approximately 250 km closer to the sun.

## VI. Concluding Remarks

A discussion of the analytical and numerical techniques used in obtaining the ISEE-3 mission orbit has been presented. The two solutions are found to be in close agreement. The maximum differences in the position components were shown to be the same order of magnitude as the truncation error in the third-order development. Stationkeeping simulation data indicated that fuel costs for halo orbit maintenance would be lowered if the spacecraft were controlled to the numerically generated orbit. This has, in fact, proved to be the case. At the time of this writing, the

ISEE-3 spacecraft was nearing completion of its third revolution in halo orbit. Stationkeeping $\Delta V$ costs for halo orbit maintenance have been averaging about 10 m/s/yr. As explained in Ref. 7, the spacecraft is controlled loosely to a toroidal region of space which surrounds the numerically generated halo orbit. An indication of the $\Delta V$ requirements vs deviations from the nominal orbit can be found in Table 6 of Ref. 7. These projections have been shown to be quite accurate when compared with data obtained from actual mission maneuvers. Since a $\Delta V$ budget of approximately 150 m/s was initially reserved for stationkeeping maneuvers, the current strategy is expected to maintain the spacecraft in halo orbit well past the NASA mission lifetime target of 5 yr.

## References

[1] Szebehely, V., *Theory of Orbits,* Academic Press, New York, 1967, Chap. 5..

[2] Richardson, D., "Periodic Orbits About the $L_1$ and $L_2$ Collinear Points in the Circular-Restricted Problem," Computer Sciences Corp. Rept. CSC/TR-78/6002, 1978.

[3] Richardson, D., "A Note on a Lagrangian Formulation for Motion About the Collinear Points," *Celestial Mechanics,* in press.

[4] Farquhar, R., "The Moon's Influence on the Location of the Sun-Earth Exterior Libration Point," *Celestial Mechanics,* Vol. 2, 1970, pp. 131-133.

[5] Brouwer, D. and Clemence, G., *Methods of Celestial Mechanics,* Academic Press, New York, 1961, pp. 308-310.

[6] Farquhar, R., Muhonen, D., and Richardson, D., "Mission Design for a Halo Orbiter of the Earth," *Journal of Spacecraft and Rockets,* Vol. 14, March 1977, pp. 170-177.

[7] Farquhar, R., Muhonen, D., Newman, C., and Heuberger, H., "The First Libration Point Satellite: Mission Overview and Flight History," AAS Paper 79-126, 1979; reprinted in this issue of *Journal of Guidance and Control* (Vol. 3, Nov.-Dec. 1980), pp. 549-554.

[8] Richardson, D., "Analytical Construction of Periodic Orbits About the Collinear Points," *Celestial Mechanics,* in press.

[9] Dasenbrock, R., "Algebraic Manipulation by Computer," U.S. Naval Research Lab. Rept. No. 756U, 1973.

[10] Farquhar, R. and Kamel, A., "Quasi-Periodic Orbits About the Trans-Lunar Libration Point," *Celestial Mechanics,* Vol. 7, 1973, pp. 458-473.

[11] Conte, R. and deBoor, C., *Elementary Numerical Analysis,* McGraw-Hill, New York, 1972, pp. 290-293.